Design and performance analysis of explosion vents: effects of groove depth and number of petals

Mithilesh Neve[1, 3 *], *Laxmi* Mulik [4], *Kaushik* Sawale[1], *Sakshi* Lanjile[1], *Naresh* Jaiswal[1], *Abhishek* Kanaskar[2], and *Ismail* Mulani[2]

[1]PVG's College of Engineering and Technology & GKPIOM, Pune-09, India
[2]Research & Development Establishment (Engrs.), DRDO, Pune-15, India
[3]Lancaster University, Lancaster LA1 4YW, United Kingdom
[4]Balmer Lawrie (UAE) LLC, Dubai, UAE

Abstract. Explosion vents, or rupture discs, are critical safety components in high-thrust article containers, ensuring controlled pressure release during operation and maintaining structural integrity of the containers. This study examines the design and performance of explosion vents, emphasizing on the effects of groove depth and petal configuration. Grooves enable precise vent opening under high-pressure conditions. Several vent variants were designed, and explicit dynamic finite element analysis (FEA) using ANSYS was performed to determine burst pressure and burst time under specified operating conditions. Mesh refinement played a key role, with a hex-dominant meshing strategy employed to enhance accuracy and computational efficiency, minimizing tetrahedral and pyramidal elements which increased geometric stiffness and compromised precision. Results showed an inverse relationship between groove depth and burst pressure, where small changes significantly impacted performance. While petal configuration had no effect on burst pressure, it caused minor variations in burst time due to stress distribution differences from impulsive loading. Minor discrepancies between theoretical and analytical results were linked to the exclusion of groove number and groove depth in calculations. This research advances the theoretical understanding of explosion vent mechanics and provides practical design guidelines for safer, more reliable explosion vents in aerospace and high-pressure storage systems.

Keywords: Rupture discs, FEA on Rupture Discs, Explosion vents, Design of Rupture Discs.

[*] Corresponding author: mithineve@gmail.com

1 Introduction

Explosion Vents are vital pressure relief devices widely used in industries like chemical manufacturing and aerospace. They are also known as rupture discs. These systems protect equipment and workers from excessive internal pressures caused by explosions or uncontrolled process conditions. Explosion vents function as weak spots in enclosures, designed to open when a specific pressure threshold is exceeded, thereby providing a controlled escape route for flames and pressure. They come in various shapes and sizes, such as domed, square, rectangular, and circular, and are typically constructed from scored metal sheets for precise and controlled rupturing.

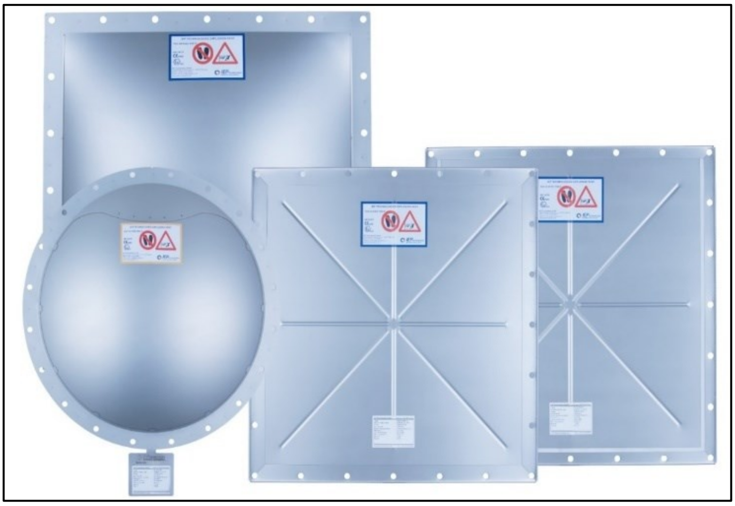

Fig. 1. Explosion vents in different shapes [1]

Application and Significance. The developed rupture disc serves as a critical safety mechanism at the rear-end of an article container. Its purpose encompasses two key aspects: providing a leak-proof seal which can sustain storage pressure and relieving pressure just above the storage pressure.

(a) As a leak-proof seal. Article containers store and secure articles under constant pressure, ensuring stability during extended storage and transport. To sustain a steady internal pressure, gases such as helium or nitrogen are used. This ensures smooth flow of the fuel and oxidizer into the combustor without direct contact between them [2]. This prevents pressure drops, safeguarding the usability of the propellant and protecting the container and its components from damage. Rupture discs act as a reliable, leak-tight barrier, withstanding constant internal pressure effectively.

(b) As a device for relieving pressure. During launch, the sudden pressure surge caused by plume release necessitates the rupture disc to fail at a pressure just above the storage level. It must respond quickly and endure high temperatures, ensuring controlled pressure relief and the safety of the system.

Among the available existing studies on explosion vents, Murty et al. [3] tried to contrast experimental data with the values acquired using FEA for a flat rupture disc. Lanjile et al. [4] provides a brief overview of the methodology used for the rupture disc. The paper observes that the pressure withstanding capacity of the rupture disc becomes greater as it deflects. Therefore, non-flat geometries are stronger and can withstand greater pressures. The disc material exhibits a non-linear behaviour.

Gupta & Nagesh [5] analysed how the thickness of a circular plate influences its tearing behaviour and overall deformation when subjected to sudden, impulsive loads. They inspected possible failure modes such as considerable permanent bending without any material rupture, splits from excessive tension, and shearing or tearing at the support points. Plates tear at their boundaries because the intense bending creates concentrated strain. When the tearing happens rapidly, the plates near the edges may not have enough time to fully deform before breaking apart.

Colombo et al. [6] used a finite element approach on different models of scored plates with varying thicknesses and groove depths to predict their behaviour and the burst pressure. Both experimental and numerical findings show that thicker plates tend to exhibit less stable tear propagation. This leads to uneven, asymmetric deformations in regions where they fail. This irregularity in symmetry is less suitable for safety-critical situations. To ensure the plate fails along the scored section, the groove depth should be at least 40% of the plate's thickness.

Georgia [7] provided comprehensive information and instructions on selection of rupture discs. Domed discs are highly stable and resist bending or warping, particularly under heavy loads. They can withstand steady system pressures up to 80% of their rated burst pressure. However, as the diameter or operating temperature increases, the burst pressure may decrease [8]. Scored forward acting (SFA) discs reduce fatigue and creep of the material during tensile loading. They allow for pressures of up to 85% of the designated burst pressure.

Zhu et al. [9] examined how temperature variations influence the burst pressure of rupture discs. A finite element simulation using ABAQUS was conducted on an AISI 316L disc to assess how plastic strain develops throughout the structure. Experimental findings in the paper revealed that the maximum burst pressure decreased progressively as the temperature rose. Fracture patterns revealed that strain hardening also becomes more pronounced with rise in temperature.

Kanakadandi, et al.[10] investigated the deformation characteristics and failure response of a thin, domed and scored metallic rupture disc subjected to storage pressure in a rocket chamber, with emphasis on its reaction to a sudden impulsive load. FEA was used to study the response of the disc (ABAQUS/Explicit Version 6.14 software) and to determine the effects of geometrical parameters such as score geometry, score pattern, loading rates, diameter-to-disc thickness ratio (D/t), dome height-to-disc diameter ratio (H/D), etc., on its deformation and failure response. The sudden impact pressure is exerted on the concave surface of the disc. Failure begins at the centre of the disc (region with highest strain concentration) in the region with scores and is disseminated along the score, until the metallic domed disc's outer boundary. However, at low loading rates, failure initiates around one-fourth of the disc's radius. The scores were made on the metallic disc's convex side. The rupture behaviour is highly susceptive of loading rates below 100 MPa/s. Beyond this threshold, responses like failure time, burst pressure, and strain distribution become relatively stable and insensitive to further increases in the loading rate.

Yu et al. [11] determined how different materials react to the bulge process for rupture discs. In this process, pre-bulging of the disc is done by application of pressure on one side. The disc gradually takes on a dome-like shape as the material deforms due to the plastic deformation. Its bulge height increases with the increase of bulge pressure in a linear manner.

This present research examines the design and analyses the performance of explosion vents under high pressure loading conditions, focusing on the effects of varying groove depths and the no. of fragments on the disc (petal configuration). The research aims to find out the burst pressure values as well as the time required for the vent to burst open (burst time), which is a differentiating factor. The focus was to achieve a controlled opening of the vent within a couple of seconds to prevent physical damage due to excess pressure in the article container. In contrast to prior studies where pressure was applied to the convex surface, the present work investigates loading conditions on the concave side of the disc, with grooves likewise machined on this surface. The disc will be manufactured out of Aluminium Alloy 1200 (H14 grade) due to its moderate strength and corrosion resistance properties. Finite element analysis using the explicit dynamics method in ANSYS software were employed to determine the burst pressure and burst time as per prescribed operational conditions, where the mesh refinement was of pivotal influence to obtain accurate results and enhance computational efficiency.

2 Methodology

The objective of this study is to focus on two variables in designing the rupture disc, namely groove depth and number of petals. After selecting a suitable material and geometry for optimal performance and manufacturability of the rupture disc and back it with finite element analysis, it will ultimately satisfy the objective of minimizing the disc's burst time and burst pressure. The primary task was to design and analyse an explosion vent (rupture disc) for an article container. The design is aimed at ensuring failure at precise pressure levels in a controlled manner (along the grooves), with minimal safety margins. The scope of the work had two major points namely –

1. **Analytical Calculations.** Exploration of material properties, determine dimensions, geometry, and safety limits for actual operating conditions.
2. **Engineering Design and Simulation Using (CAD) and (FEA) Tools.** Employ software tools like SolidWorks 2022 and ANSYS R1 2022 to create and evaluate models.

There are two variables considered in this study which include - Number of Petals (refer to the segments in the rupture disc that are separated by scored lines, which influence the pattern and efficiency of rupture under pressure); and Depth of Notch or Groove Depth (refers to the depth of the scored lines, which directly affects the pressure at which the disc bursts).

There were some predefined assumptions and constraints which have been considered during the research. Firstly, the factor of safety should be kept as low as possible, ideally approaching zero to ensure that the rupture disc fails precisely at the desired pressure. Secondly, the influence of temperature and the back pressure generated within the article container after propulsion of gases are to be neglected.

2.1 Design Process

A detailed design process is followed which involved evaluation of factors such as the intended application, pressure applied, material selection, and operating conditions. The appropriate dimensions and material of the rupture disc are to be determined before proceeding on to the FEA. The design was constrained by predefined parameters, specifically a disc diameter of 325 mm and a storage pressure of 0.2 barg within the article container.

2.2 Material Selection

The material of a rupture disc directly impacts its ability to effectively respond to fluctuations in pressure. Different materials offer different degrees of resistance to pressure, temperature, corrosion, and to premature failure. Two materials were considered namely AA 1200 H14 and AA 1100 – O. The material properties of these two are derived from ANSYS Material Library and are shown in the Table 1 below.

Table 1. Mechanical and Thermal properties of Materials

Property	AA 1200 H14	AA 1100 – O
Ultimate Tensile Strength, σ_{us} (MPa)	124.9	89.6
Thermal Conductivity (W/m-K)	230	222
Yield Strength (MPa)	114.8	25
Elongation at break, δ (%)	5.1	15 - 28
Poisson's ratio	0.3333	0.3333
Elastic Modulus (GPa)	69	69

After studying the material properties, AA 1200 H14 was finalized for manufacturing the rupture disc. AA 1200 H14 is a cost-effective material for rupture discs. It exhibits a reasonable elongation at break (5.1%) and its ultimate tensile strength is neither too high nor too low (124.9 MPa). While AA 1200 H14 is not as corrosion-resistant as some other alloys, it still offers good resistance to atmospheric corrosion.

2.3 Calculations

The pressure a disc can handle before bursting is related to the material's ultimate tensile strength, as given by [12] –

$$P_b = \frac{2\, t\, \sigma_{us}}{R}, \tag{1}$$

$$P_b = \frac{8\, t\, \sigma_{us}}{D} \sqrt{\frac{1+\frac{\delta}{100}}{\sqrt{1+\frac{\delta}{100}}-1}}. \tag{2}$$

Some design considerations were taken into account following the results obtained in [6, 9]. These are as follows –

$$\frac{D}{t} > 100, \tag{3}$$

$$\frac{t_1}{t} \geq 0.4, \tag{4}$$

such that the failure will occur in the grooved region.

Given: D = 325 mm, Storage Pressure = 0.2 barg.

To find – $t,\ t_1,\ P_b,$ and R.

Assumption – The material used is AA 1200 H14.
Using Eq. 3 we get, $t < 3.25$ mm

$\therefore t = 1.5$ mm (assumption).

Using Eq. 4, we get, $t_1 \geq 0.6$ mm

$\therefore t_1 = 1.3$ mm (assumption).

Therefore, considering values of σ_{us} and δ from Table 1 and Using Eq. 2, we get

$\therefore P_b = 7.271 \frac{\mathrm{kg}}{\mathrm{cm}^2} = 7.13$ barg.

Now, to consider the effect of P_b on R, we calculate the value of (R) for low gauge pressure.

If P_b = 0.3 barg, then from Eq. 1,

$\therefore R = 19119.675$ mm.

For the given diameter D = 325 mm, the value of R obtained above is sufficiently high, so it may be assumed that R tends to infinity. This means that only a flat disc would burst around P_b = 0.3 barg pressure which is above storage pressure 0.2 barg. Hence, it was designed and analysis was conducted.

2.4 CAD Model Development

After completing the material selection and theoretical calculations, the CAD model of the rupture disc was developed using SolidWorks software to ensure precision and adaptability for further analysis. The rupture disc's central diameter was defined as 325 mm, while the total diameter was set at 390 mm. The plate thickness was derived from theoretical calculations and determined to be 1.5 mm, ensuring structural integrity and compatibility with the operational load conditions. The groove depth, a critical parameter influencing the venting efficiency, was calculated as 1.3 mm. The grooves made on the disc are of triangular geometry (isosceles triangle). The number of petals, critical for ensuring controlled rupture during operation, were assumed to be four and six based on design considerations [10]. These inputs were systematically incorporated into the CAD model, capturing all geometric and functional attributes necessary for subsequent analysis. The dimensions and parameters described above correspond to Disc A, while Disc B and Disc C were additionally developed by varying the groove depth (i.e. 1 mm) and the number of petals (i.e. 6) to evaluate their influence on rupture performance.

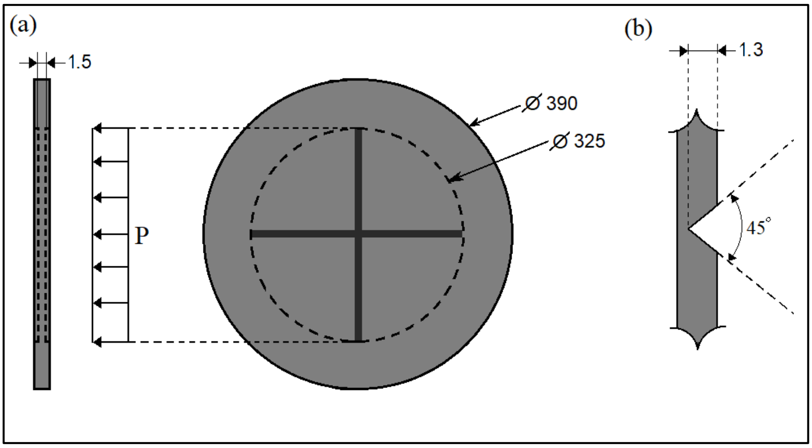

Fig. 2. Disc Dimensions

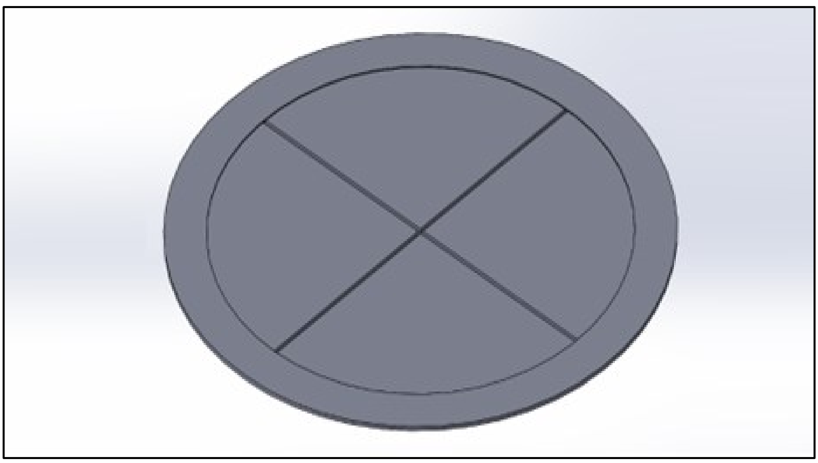

Fig. 3. CAD Model for Circular Flat (Disc A)

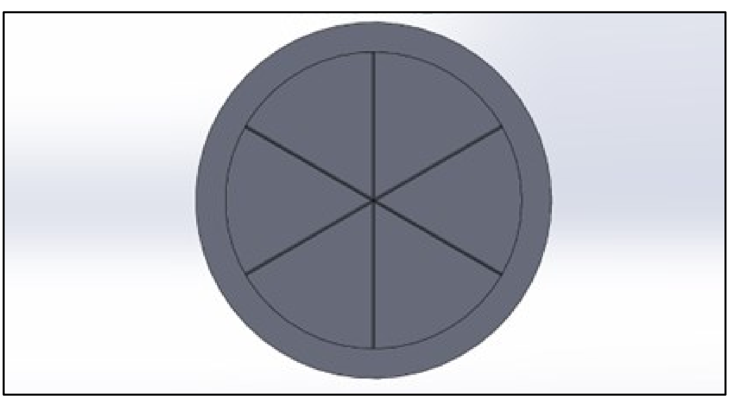

Fig. 4. CAD Model for Circular Flat (Disc C)

2.5 Finite Element Analysis

It is a discretization-based method that approximates solutions for engineering and physics problems while minimizing errors [13]. It can be used to analyse the dynamic transient response of rupture discs under various scenarios. Using ANSYS, it was examined how burst behaviour changes with different parameters.

2.5.1 Explicit Dynamic Analysis

Explicit dynamic analysis simulates structural behaviour under dynamic loads such as impacts, blasts, or crashes. Unlike implicit methods, it directly integrates equations of motion over small-time steps to model transient phenomena. This method is ideal for scenarios with rapidly varying loads, such as stress and shock wave formation, material deformation, and failure at high strain rates during crashes, impacts, or blasts [14]. Applications include short-duration dynamic events, wave propagation through gases, liquids, and solids and extreme loadings. For rupture discs, explicit dynamic analysis provides insights into behaviour under tensile stresses (forward-acting discs) or buckling (reverse-acting discs) and effectively captures nonlinear, short-duration dynamic loading scenarios. Also, it possesses the ability to simulate the actual behaviour under applied loading conditions along with visualization of the bursting phenomenon.

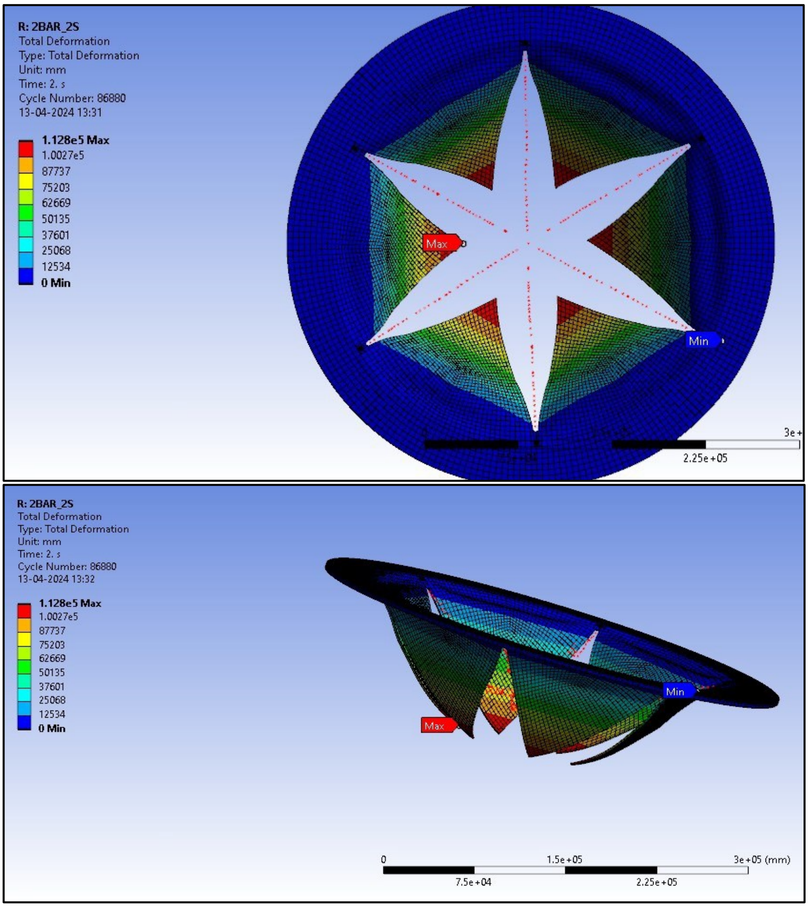

Fig. 5. Bursting of Disc C

2.5.2 Meshing

A good quality mesh, having uniform pattern, element size and shape, plays an important role in obtaining accurate and reliable results. Refined meshes can capture detailed geometric features and yield more accurate results, while coarse mesh may overlook critical information. Hence, the mesh density greatly affects the accuracy of the analysis. Additionally, a well-refined mesh aids in ensuring solution convergence, particularly for highly nonlinear or dynamic problems. Mesh density directly influences computational cost. Therefore, mesh density must be carefully balanced according to the problem's complexity and the required level of precision.

Mesh refinement should focus on regions of interest, such as areas with high stress concentrations or applied boundary conditions. For rupture discs, stress concentrations are typically observed in the grooved region, characterized by intricate geometry and minimal thickness. This complexity can result in the formation of tetrahedral and pyramidal elements, which are undesirable due to their reduced accuracy. To address this, finer mesh sizing is applied selectively in such areas to accurately capture stress distribution and deformation.

2.5.3 Mesh Optimization

Upon identifying discrepancies between theoretical and analytical results, mesh properties were systematically optimized. Closer examination revealed that tetrahedral and pyramidal elements are concentrated near the grooved region leading to unnecessary stiffness to the geometry and eventually increasing the burst pressure to 20 barg (performed and then documented). It is well-documented that tet-dominant mesh yield less accurate results compared to hexahedral elements [15]. While tetrahedral elements are suitable for geometries with intricate curves and acute angles where hex mesh is impractical, hexahedral elements are preferred due to their superior computational and numerical efficiency in finite element analysis (FEA).

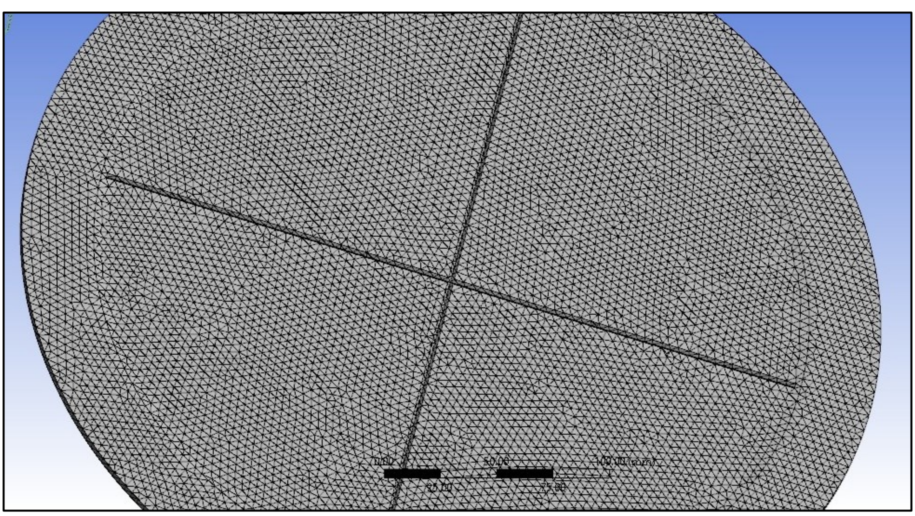

Fig. 6. Tetrahedral Mesh for (Disc A)

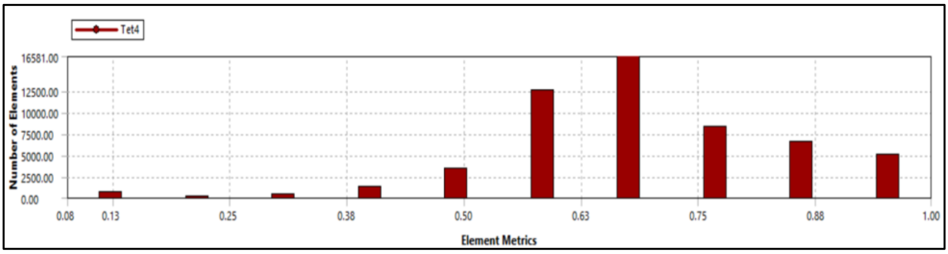

Fig. 7. Element Metrics for (Disc A)

A hybrid meshing approach was adopted with 4 mm element size, combining hex-dominant mesh in 95% of areas with tetrahedral elements in areas where hex elements were ineffective. Research indicates that tetrahedral, pyramidal, and triangular elements significantly increase stiffness in the model, contributing to initial deviations in the analysis [16-17]. To mitigate this, the proportion of these elements was limited to less than 5% of the total mesh and avoided in critical regions, ensuring improved accuracy and reliable simulation results.

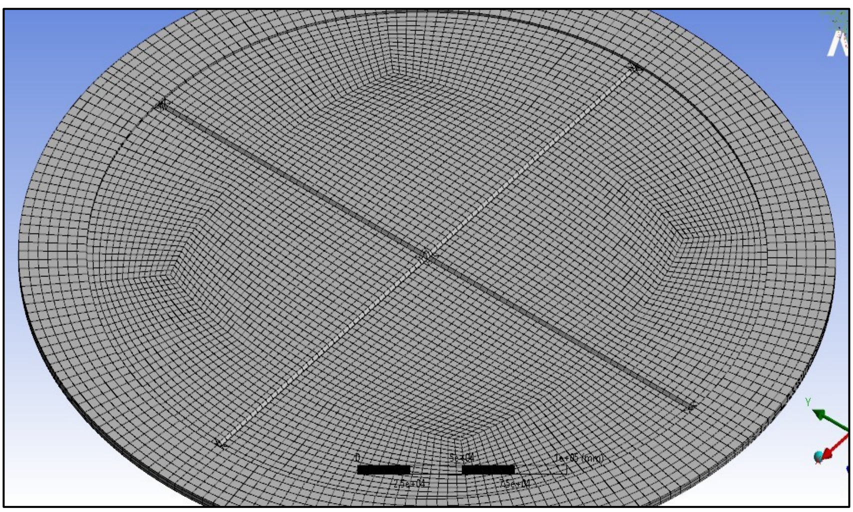

Fig. 8. Hexahedral Mesh for (Disc A)

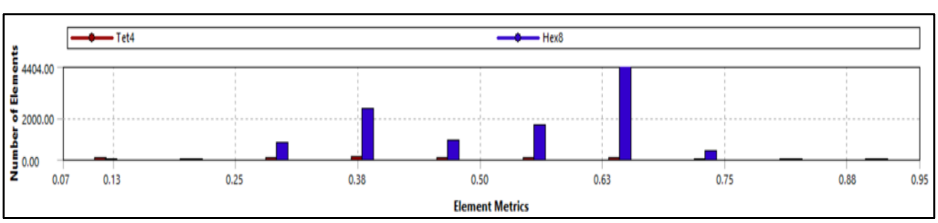

Fig. 9. Mesh Metrics for (Disc A) (Blue – Hex elements, Red – Tet elements)

To summarise, a CAD model of the disc was loaded into ANSYS with an appropriate material. The model was meshed and the collars of the disc were given fixed boundary conditions. Initial results required mesh refinement to address inaccuracies caused by tetrahedral elements. After optimizing the mesh, consistent results were achieved, confirming the disc's burst pressure just above the storage pressure (0.2 barg). Further evaluations considered variable effects on performance. This systematic methodology ensures a thorough analysis and optimized design for the rupture disc, aligning with project objectives and operational requirements. Failure of the rupture disc was observed, which initiated at its centre and propagated towards circumference of disc and assured controlled failure along the grooves.

3 Results

3.1 Circular Flat Disc A

Table 2. Results for (Disc A)

Material	AA 1200 H14
Mesh Nodes	18870
Mesh Elements	10912
Disc Thickness (mm)	1.5
Mesh Element Size (mm)	4
Groove Depth (mm)	1.3
No. of Petals	4
Groove Angle (°)	45
Burst Pressure (barg)	0.3
Max Deformation (mm)	15242
Max Stress (MPa)	118.96
Peak stress at burst initiation (MPa)	115.93 at 1.5354 (sec)
Time to burst (sec)	1.5556
Failure initiation location	Centre of disc

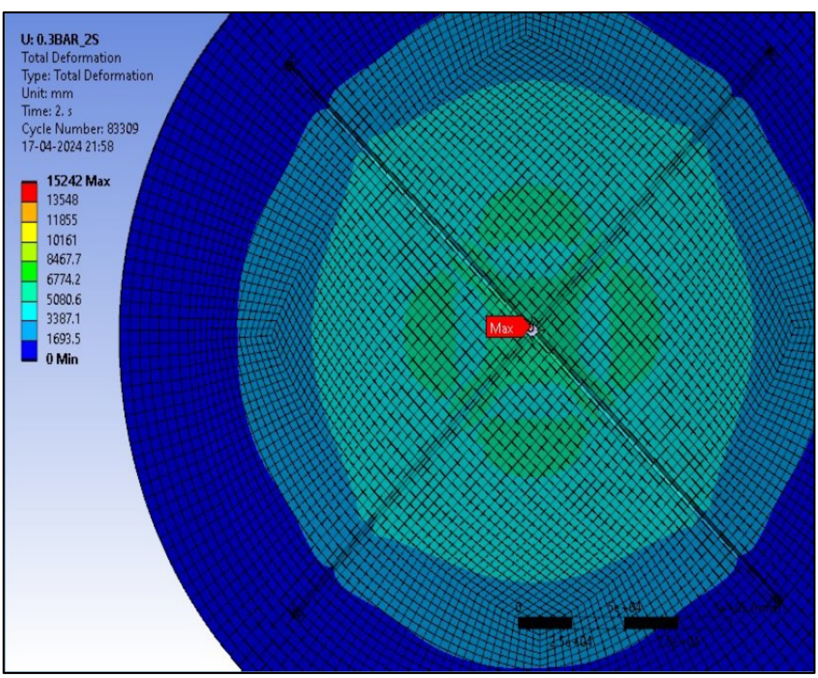

Fig. 10. Total Deformation (Disc A, 0.3 barg)

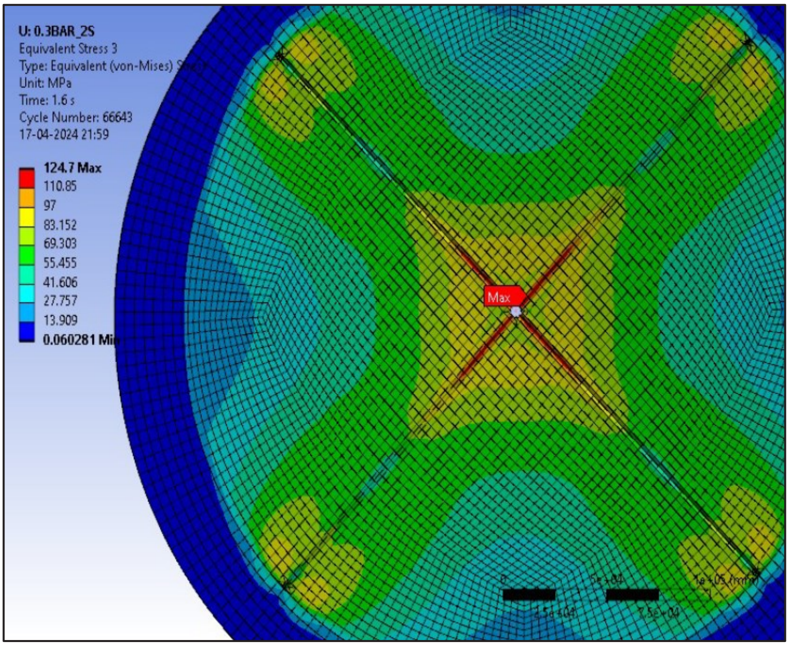

Fig. 11. Equivalent Stress Distribution Post-Burst (Disc A, 0.3 barg)

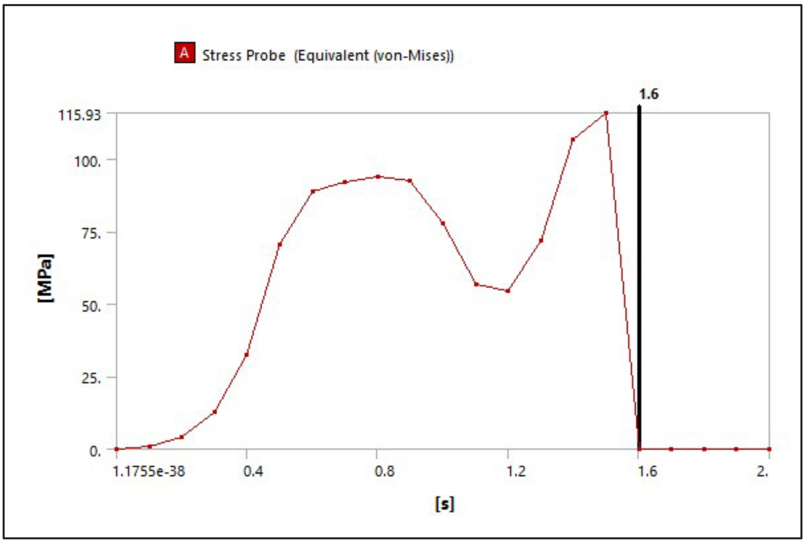

Fig. 12. Stress Probe at Centre (Disc A, 0.3 barg)

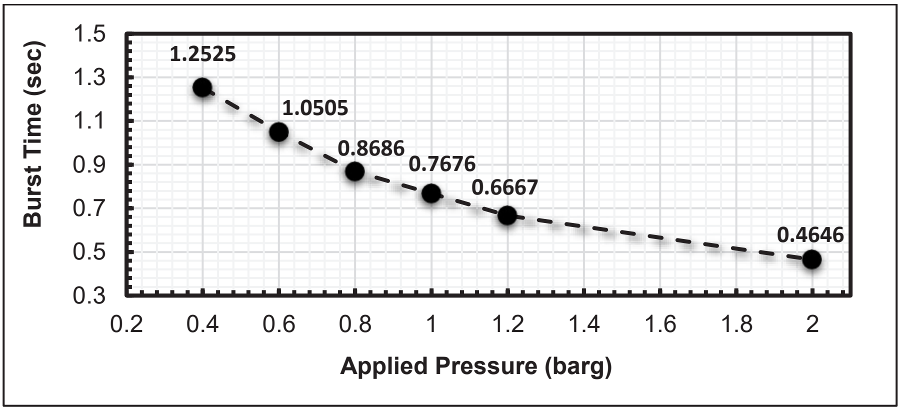

Fig. 13. Graph showing the Burst Time at corresponding Burst Pressure (Disc A)

The graph in the Fig. 13 illustrates the relationship between applied pressure and burst time, showcasing a clear inverse trend. As the applied pressure increases, the burst time decreases consistently. At an applied pressure of 0.4 barg, the burst time is at its maximum of 1.2525 seconds, indicating a slower rupture response. With increasing pressure, the burst time reduces progressively, reaching 0.8686 seconds at 0.8 barg and further decreasing to 0.6667 seconds at 1.2 barg. At the highest pressure of 2.0 barg, the burst time drops to its minimum of 0.4646 seconds. This trend signifies that higher applied pressures accelerate the rupture process. Similar trend was observed for the other two-disc variants (B and C). The graphs for these variants are shown in the following section.

3.2 Circular Flat Disc B

Table 3. Results for (Disc B)

Material	AA 1200 H14
Mesh Nodes	18870
Mesh Elements	10912
Disc Thickness (mm)	1.5
Mesh Element Size (mm)	4
Groove Depth (mm)	1
No. of Petals	4
Groove Angle (°)	45
Burst Pressure (barg)	1.4
Maximum Deformation (mm)	16883
Maximum Stress (MPa)	109.58
Peak stress at burst initiation (MPa)	11.828 at 1.6364 (sec)
Time to burst (sec)	1.6566
Failure initiation	Centre of disc

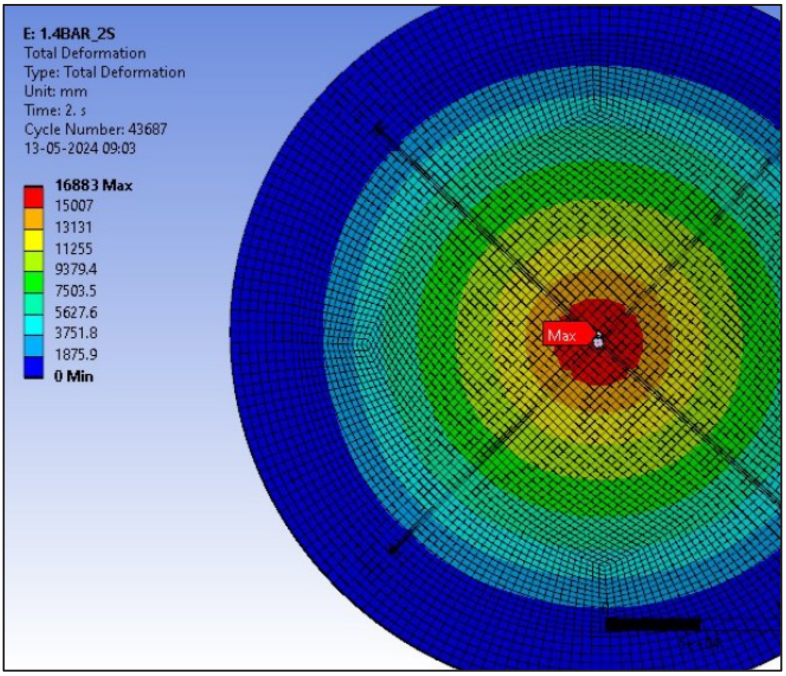

Fig. 14. Total Deformation (Disc B, 1.4 barg)

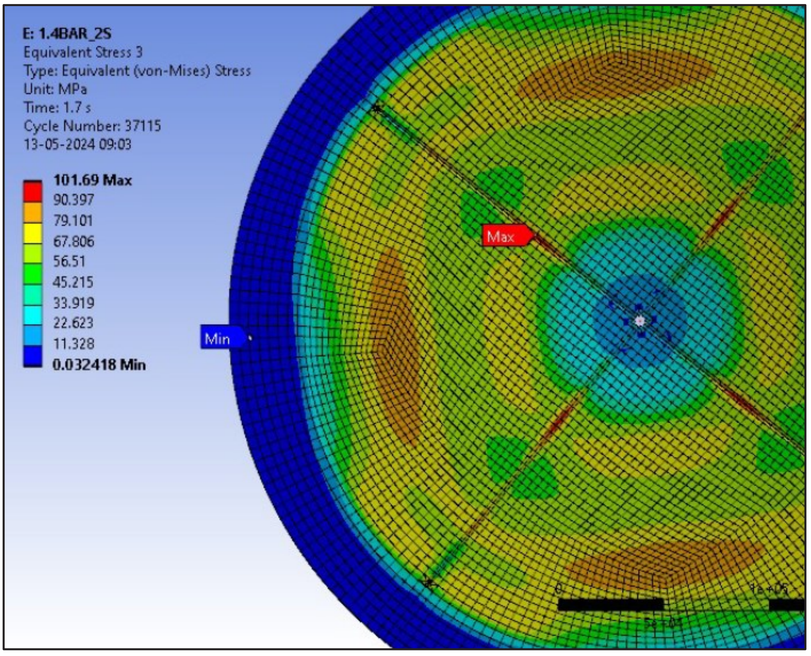

Fig. 15. Equivalent Stress Distribution Post-Burst (Disc B, 1.4 barg)

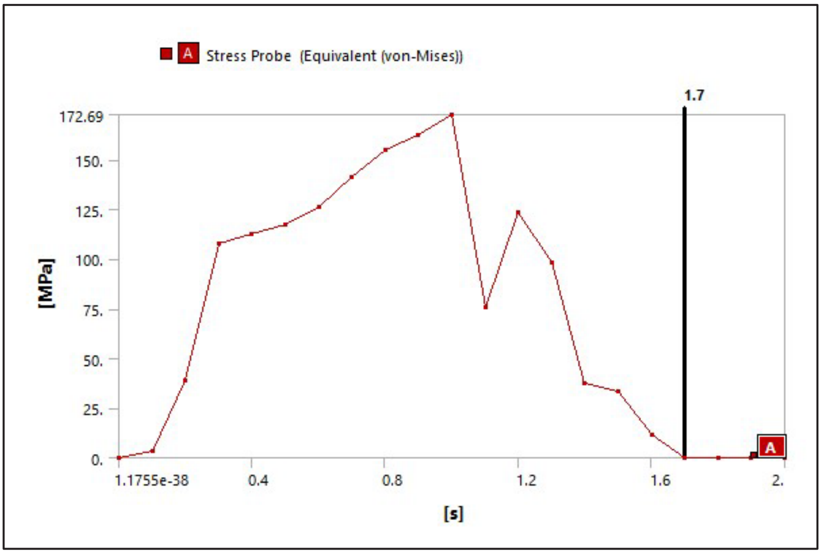

Fig. 16. Stress Probe at Centre (Disc B, 1.4 barg)

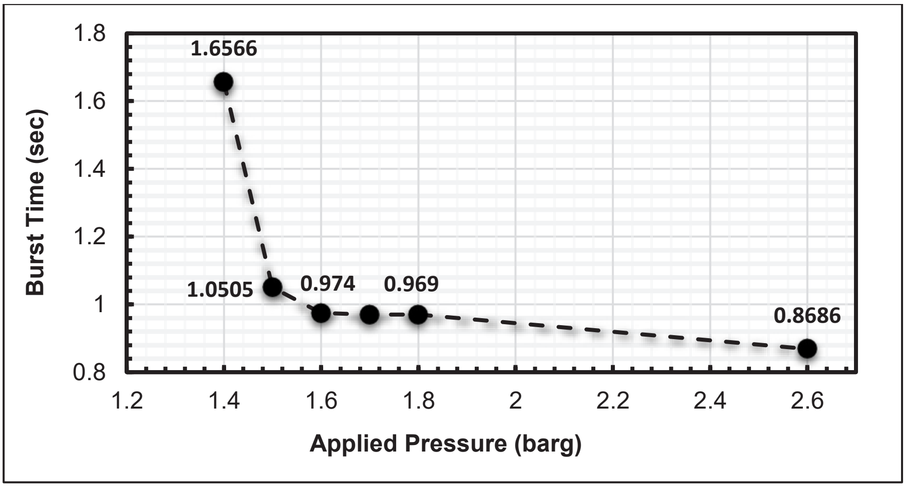

Fig. 17. Graph showing the Burst Time at corresponding Burst Pressure (Disc B)

3.3 Circular Flat Disc C

Table 4. Results for (Disc C)

Material	AA 1200 H14
Mesh Nodes	21410
Mesh Elements	12450
Disc Thickness (mm)	1.5
Mesh Element Size (mm)	4
Groove Depth (mm)	1.3
No. of Petals	6
Groove Angle (°)	45
Burst Pressure (barg)	0.3
Maximum Deformation (mm)	12884
Maximum Stress (MPa)	120.13
Peak stress at burst initiation (MPa)	120.13 at 1.6364 (sec)
Time to burst (sec)	1.6566
Failure initiation	Centre of disc

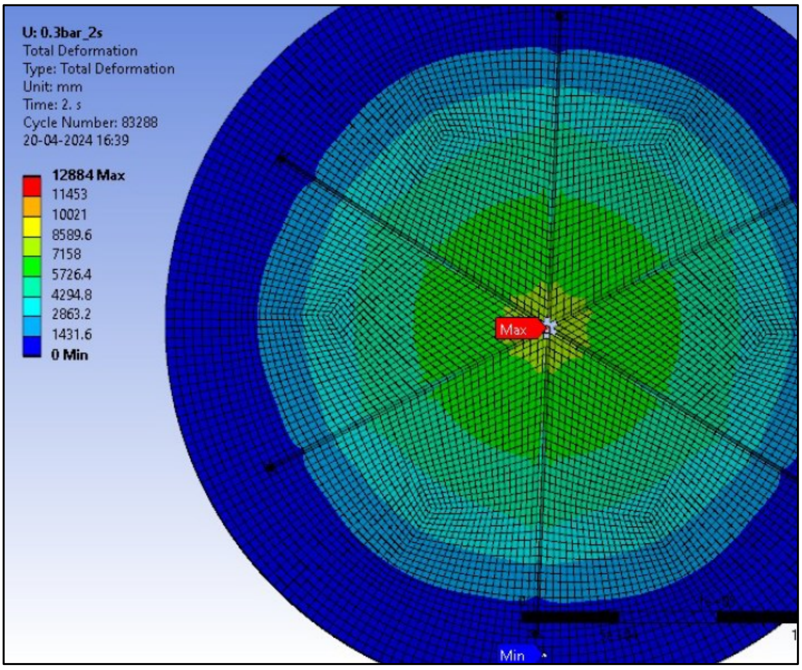

Fig. 18. Total Deformation (Disc C, 0.3 barg)

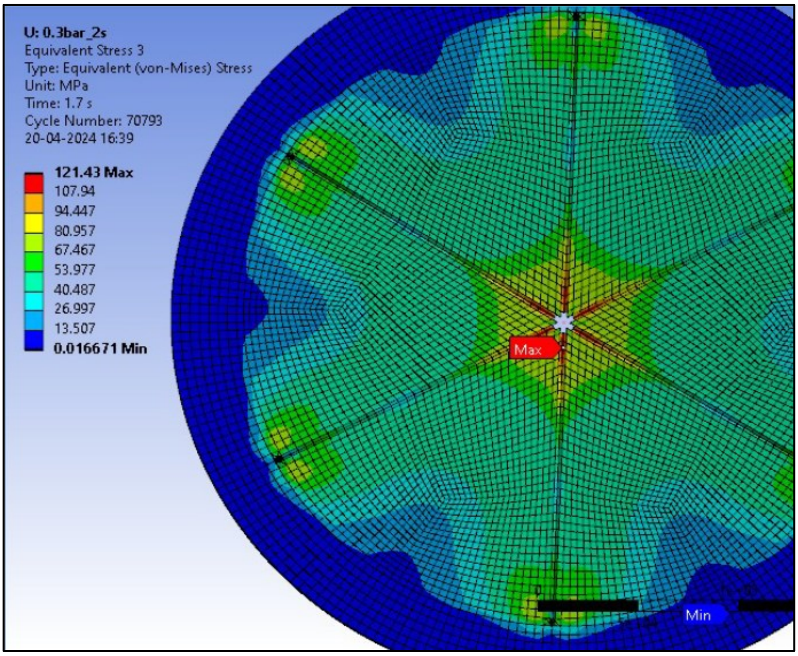

Fig. 19. Equivalent Stress Distribution Post-Burst (Disc C, 0.3 barg)

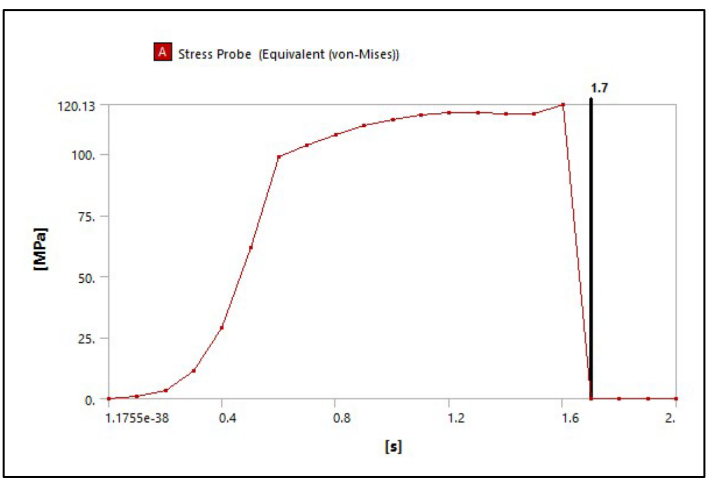

Fig. 20. Stress Probe at Centre (Disc C, 0.3 barg)

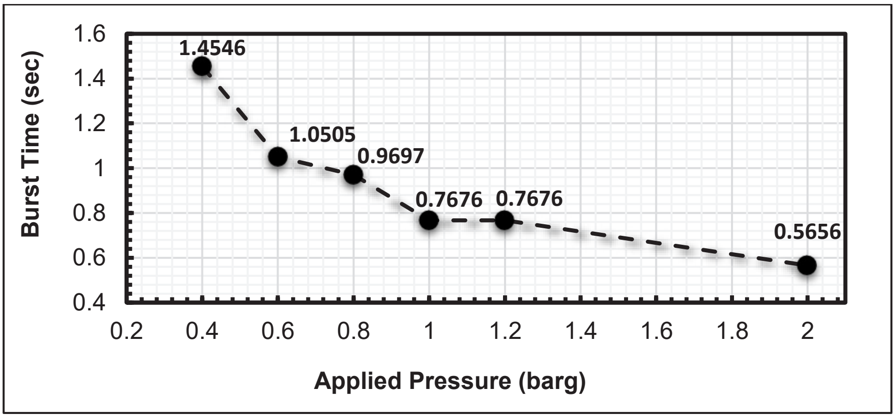

Fig. 21. Graph showing the Burst Time at corresponding Burst Pressure (Disc C)

4 Discussion

The influence of the two variables examined in this study on the rupture disc's burst pressure and burst time is discussed below –

Table 5. Influence of Groove Depth on Burst Pressure and Burst Time of Rupture Disc

Fixed Variables	Rupture Disc Variants	Varying Groove Depth [mm]	Burst Pressure [barg]	Burst Time [sec]	Relative Groove Depth (t_1/t)
N = 4, t = 1.5 mm,	Disc A	1.3	0.3	1.5556	0.866
	Disc B	1	1.4	1.6566	0.666

The groove depth is inversely proportional to burst pressure. It was observed from the Table 5 that as the ratio of relative groove depth (t_1/t) approaches 1, burst pressure decreases. However, the ratio (t_1/t) should always lie in between 0.4 to 1. If the ratio exceeds 1 the grooves will be converted to slits. Hence, a small change in the groove depth affects the burst pressure significantly.

Table 6. Influence of Number of Petals on Burst Pressure and Burst Time of Rupture Disc

Fixed Variables	Rupture Disc Variants	Varying No. of Petals	Burst Pressure [barg]	Burst Time [sec]	Difference in Burst Time [sec]
t = 1.5 mm, t_1 = 1.3 mm	Disc A	4	0.3	1.5556	0.1
	Disc C	6	0.3	1.6566	

The data presented in the Table 6 indicates that the number of petals does not influence the burst pressure. However, it impacts the burst time, with a difference of 0.1 seconds was observed. This behaviour can be explained using the relationship, (Pressure = Force / Area).

A six-petal disc has a slightly larger surface area compared to a four-petal disc. To maintain a constant pressure, an increase in area necessitates a decrease in force per unit area.

As a result, force spreads over a wider area for the six-petal disc, due to which stress concentration is reduced and the burst time is delayed.

Conversely, in the case of the four-petal disc, the force is concentrated over a smaller area, leading to higher localized stress and a quicker rupture. This distinction highlights the role of petal configuration in influencing the burst time while maintaining consistent burst pressure.

5 Conclusion

This study investigates the bursting behaviour of rupture discs, essential safety components in the chemical and aerospace industries, particularly for high-thrust article containers. These discs ensure controlled pressure release while maintaining a leak-proof seal under storage conditions and facilitating pressure relief marginally above storage pressure. Theoretical design calculations determined the disc dimensions, and explicit dynamics simulations in ANSYS were conducted on three CAD-model variants subjected to impulsive loading. The objectives of minimizing burst time and achieving a burst pressure slightly above storage pressure were successfully met, with simulation results aligning well with the intended design goals.

Key conclusions derived from this study include:

1. *Material Selection*: Aluminium Alloy 1200 (H14 grade) is an optimal choice due to its moderate tensile strength, resistance to corrosive and toxic fluids, and cost-effectiveness.
2. *Groove Depth*: The groove depth-to-disc thickness ratio (t_1/t) should be in between 0.4 to 1. The burst pressure is inversely proportional to (t_1/t). Thus, a minor difference in the depth of the groove significantly affects the rupture/burst pressure.
3. *Petal Configuration*: Circular discs with four petals are preferred over six-petal variants, considering manufacturing feasibility and design complexity. The burst pressure is the same for both variants; however, the burst time varies by 0.1s due to the differences in the total surface area and values of localized stresses as a result.
4. *Theoretical vs. Analytical Discrepancy*: Variations in results arose because of the exclusion of two parameters, groove number and groove depth in theoretical calculations.
5. *Mesh Optimization*: Dominance of hexahedral elements (95%) in the meshing process ensures high accuracy, with tetrahedral and pyramidal elements restricted to less than 5% in geometrically challenging areas.

Future research may explore the effects of disc geometry variations, pressure application direction (Applied to the same side as the grooves or to the reverse side), back-pressure from adjacent articles in stacked configurations, temperature effects due to gas propulsion on burst pressure and time and potential for exploring alternative materials.

Nomenclature

P_b = Burst Pressure of disc (barg)
t = Disc Thickness (mm)
σ_{us} = Material's Ultimate tensile strength (MPa)
t_1 = Score/groove depth (mm)
R = Radius of curvature of disc (mm)

D = Disc Diameter (mm)
N = Number of Petals
δ = Material Elongation (%)

Appendix

The Article Container. The containers are typically hollow cylindrical or rectangular cross sections that store the body of the article until it is used. They must not only be able to withstand structural loads but also pressure and thermal loads released from the rocket booster.

References

1. Information on https://www.directindustry.com/prod/iep-technologies/product-196696-2128745.html
2. Parks, J. S., Practical applications of pressure-fed LOX/CH4 rocket engines. University of Texas at El Paso (2022).
3. Murty, D. V. R., & Rao, Y. B., Computer Simulation of Rupture Disc Design. Volume 3: Design and Analysis (2006). https://doi.org/10.1115/pvp2006-icpvt-11-94060
4. Lanjile, S., Mulik, L., Neve, M., Sawale, K. and Jaiswal, N., An Overview of Design and Validation of Explosion Vents. International Journal of Scientific Research and Engineering Development, [online] 7 (2024). https://ijsred.com/volume7/issue2/IJSRED-V7I2P117.pdf
5. Gupta, N. K., & Nagesh, Deformation and tearing of circular plates with varying support conditions under uniform impulsive loads. International Journal of Impact Engineering, 34(1), 42–59 (2007). https://doi.org/10.1016/j.ijimpeng.2006.05.002
6. Colombo, M., Martinelli, P., & di Prisco, M., Validation of a computational approach to predict bursting pressure of scored steel plates. Experimental Mechanics, 54(9), 1555–1573 (2014). https://doi.org/10.1007/s11340-014-9916-9
7. Georgia, R., *ZOOK metal rupture disk public handbook 2018*. Zookdisk.com. (2018). https://marketingportal.zookdisk.com/download/zook-metalrupturedisk-public-handbook-2018/
8. Mohebbi, M., Panahizadeh, V., & Hoseinpour, M., Analytically predicting the burst pressure of composite rupture discs by considering nonlinear strain path. *Proceedings of the Institution of Mechanical Engineers, Part B: Journal of Engineering Manufacture*, *237*(1–2), 171–180 (2023). https://doi.org/10.1177/09544054221100324
9. Zhu, H., Xu, W., Luo, Z., & Zheng, H., Finite element analysis on the temperature-dependent burst behavior of domed 316L austenitic stainless steel rupture disc. Metals, 10(2), 232 (2020). https://doi.org/10.3390/met10020232
10. Kanakadandi, G., Narayanamurthy, V., & Rao, Y. V. D., Deformation and failure of thin domed-scored metallic disc under impulsive loading. International Journal of Protective Structures, 14(2), 185–220 (2023). https://doi.org/10.1177/20414196221095249
11. Yu, X., Yan, X., Li, Y., Zeng, F., Kang, S., & Yu, J., Determination of the plastic stress–strain relationship of a rupture disc material with quasi-static and dynamic pneumatic

bulge processes. Processes (Basel, Switzerland), 10(8), 1463 (2022). https://doi.org/10.3390/pr10081463

12. Vodyanik, V. I., Design of safety rupture discs. Chemical and Petroleum Engineering, 8(6), 586–588 (1972). https://doi.org/10.1007/bf01139117
13. Navin Baskar, What is Finite Element Analysis (FEA)? [online] Skill-Lync (2022). Available at: https://skill-lync.com/blogs/technical-blogs/cae-what-is-finite-element-analysis-fea
14. Information on https://www.ansys.com/en-in/blog/what-is-explicit-dynamics
15. Schneider, T., Hu, Y., Gao, X., Dumas, J., Zorin, D., & Panozzo, D., A large-scale comparison of tetrahedral and hexahedral elements for solving elliptic PDEs with the Finite Element Method. ACM Transactions on Graphics, 41(3), 1–14 (2022). https://doi.org/10.1145/3508372
16. Benzley, S., Perry, E., Merkley, K., Clark, B., & Sjaardema, G., A Comparison of All Hexagonal and All Tetrahedral Finite Element Meshes for Elastic and Elasto-Plastic Analysis. Proceedings, 4th International Meshing Roundtable, 17 (1995).
17. Krishna Kaushik Yanamundra *et al* 2018 *IOP Conf. Ser.: Mater. Sci. Eng.* 346 012075. DOI 10.1088/1757-899X/346/1/012075